Education of environmental science using a blog

Institute for Information Education, University of Edogawa, Komaki 474, Nagareyama, Chiba, Japan.

Tomoo AOYAMA[1)]

Abstract

For self-study under COVID-19, we publish an education/research blog for environmental science. The blog premise is: there is a discussion with professors such as using e-mail; and teaching materials for self-study. So, there is less description in the blog, but many images are posted. They are processed by 7 imaging-parameters, and important patterns are emphasized. We explain meanings of the parameters.

The blog has been open to public since July 14, 2020. On Jan. 8, 2021, there are over 200 articles. They are about weather, dust, sea surface anomalies, and volcanic conditions on the Earth's hemisphere that can be detected by a geostationary satellite at 140.7 degrees east longitude.

Keywords: Himawari-8, visualization, earth status, volcanoes, forest fire, sea pollution, SPM, PM2.5

1. Introduction

This is a report of liberal arts under the COVID-19 pandemic. Nowadays, it is difficult to lecture liberal arts subjects in a large classroom. There is less choice but to have students learned by themselves in internet environments and submit their reports. We can support students' self-studies; under such the view point, we propose followings.

2. Bases for learning

The environmental education requires assemble of many facts about meteorology, statistics, geology, information science, etc. It's a comprehensive science. Students must know a lot of facts far from that of mass communications means. Important facts would be hidden in many kinds of databases (DB) for the environmental science. The students have to learn how to use/analyze them. Since there are various analysis approaches, we believe it is better for us to actually analyze and exemplify environmental events using the DB. Here; we assume the following DB [1~10].

3. Our approach

We adopt a blog [11] to make the examples known to students (and graduated peoples). Blog can update itself at any time, and colors are also available. It is not appropriate for long sentences. "twitter" is also unusable in this respect; and "note" is insufficient access from search engines. Since we separate complex facts and the explanations over many articles, the defect can be reduced.

We are writing in English for attending international students and Japanese living in overseas. Characters are garbled and cannot be read from overseas unless the Japanese environment is installed. Since elementary English is used, sentences can be converted to many other languages by using translation services implemented in browsers [14]. Thus; even native Japanese grown in Japan can recognize the articles.

4. Blog

Contents of the articles are facts after 2020, which are detected from a satellite Himawari-8 that is geostationary one on latitude 140.7 deg, height 35.8km. The observing wave length is from 0.47 to 13.3 μm. Sampling interval is 10 or 2.5 [min].

Thus, time series events can be traced. Moreover, by using image processing, much invisible phenomena are detected. Followings are about already published articles. We use Japan Standard Time (JST), world time +9h; Temperature unit is Celsius. We check Himawari-8 images every day with the following areas in mind.

4.1 China

1) Status of land waters,

2) Sea surface pollution along the coast (Balhae, east China sea),

3) Haze distribution, snowfield dirt distribution; yellow sand,

2021年1月28日受付　2021年2月4日受理

1）Edogawa Univercity Institute of Information Education

4) Cloud behavior during high-concentration haze; as one interesting phenomenon, iridescent cloud phenomenon,
5) Wildfires in the southern and remote areas, that would be impacted on global warming,
6) Rains in the Taklamakan and inner Mongolia desert, vegetation time-series changes.

4.2 Russia

1) Siberian large scale forest fire, soot flow to the Arctic.

4.3 Australia

1) Black band on the Antarctic convergence line,
2) Eutrophication of the Timor Sea and northern Australia,
3) Large scale red dust flow in western Australia,
4) Northeastern wildfire,
5) The blue tide vortex of the Great Australian Bight,
6) Blue tide distribution in New Zealand waters,
7) Large forest fire in the southeast.

Forest fires and wildfires can be seen in various places on satellite images; but they are not so problematic at COP25 (2019.12). we think so strange.

4.4 India

1) Haze distribution in the east.

4.5 Volcanoes

1) Ogasawara, Nishinoshima,
2) Hawaii island, Kilauea volcano,
3) Luzon island, Taal volcano*.

Where "*" is an event happened in 2019. Volcanic eruptions are related to global climate change; thus, it cannot be overlooked.

4.6 Typhoon

We discuss it in Section 6.

4.7 Current status of the solar spherical on X-ray

The status of solar activity is related to global climate change.

4.8 Current status of the COVID-19

COVID has nothing to do with earth science; but, it has to do with how teachers conduct classes. This is the first reason mentioned in the blog. The second reason is: considering the global environment including phenomena of human society, the research belongs to a new academic field. Mathematical quantification of social phenomena requires a kind of scientific and objective index. As a response to the index, we wish to detect hidden characteristics of human society.

We consider blogs not as thesis, but as a form of preliminary discussions. Using statistical orthodox approaches, under uncertain information, i.e., daily extreme numerical fluctuations, we are trying to detect the spread phenomenon of SARS-CoV-2 virus and effects in many kinds of human society.

5. Parameterization of image processing

Himawari-8 is a satellite for the meteorological purpose; thus, clouds are detected clearly. But, under the strong clouds images, small other phenomena may be hidden. We wish to detect the hidden images. To detect many kinds of phenomena, we emphasize the originals about brightness, color, timing.

For reproducibility of the emphasis operations, operations are quantified and expressed as parameters.

5.1 Brightness

The brightness is increased or decreased by multiplying each pixel value and a positive real number given by the parameter-1. A pixel values is integer in most information engineering, which is defined by the image format. That's not enough for physically meaningful processing. We represent 1-pixel value as a 32-bit real number corresponding to 3 primary colors of RGB.

5.2 Color

We believe that any object has color components. White clouds have a white (R = G = B) part and difference parts from it. The difference parts are considered as color signals. 1 pixel is expressed by {Y(r),Y(g),Y(b)}.

$W=\min\{Y(r),Y(g),Y(b)\}$;

$dY(r)=Y(r)-W$, $dY(g)=Y(g)-W$, $dY(b)=Y(b)-W$;

$Y'(r)=Q*W+dY(r)$, $Y'(g)=Q*W+dY(g)$, $Y'(b)=Q*W+dY(b)$.

Therefore; by the Q (parameter-2), color components of {Y'(r),Y'(g),Y'(b)} is increased/decreased from that of {Y(r),Y(g),Y(b)}.

5.3 Suppression of bluish haze

The satellite image has bluish coloring. Objects having strong brightness like clouds can be identified as they are. However, patterns of ground surfaces, polluted water surfaces, volcanic plumes, and forest/wild fires are weakened by the bluish haze, and difficult to identify them. The sunlight gives a dependent scattered light X (λ) that is proportional to the nth power of wavelength (λ) by haze

particles. X (λ)=λ^{-n}, n=0 ~ 4.
The value of nth depends on the diameter of particles.
Now, let the typical wavelength of RGB be λr, λg, λb.
The brightness Y of a pixel is Y=λr^{-n} + λg^{-n} + λb^{-n}.
In case of human's eye, "λr=0.63, λg=0.55, λb=0.45 [μm]" is a standard. Thus; we multiplied 2 coefficients to GB components of each pixel. The coefficients are,
Kg=$0.55^{-n}/0.63^{-n}$, and Kb=$0.45^{-n}/0.63^{-n}$. The "n" is a parameter. Here; we write "amp=parameter-1, Q, n" as a set.

5.4 Bias

The brightness value of each pixel of an original image is depended with the position of sun. The gradient is remarkable at sunrise and sunset. Increasing the parameter-1 in Section 5.1 increases the gradient becomes noticeable. Here, the size of images is defined as 1366 * 768 pixels. A linear slope is sufficient for this size. Therefore, we introduce 3 parameters, bi, bE, and bN. They are real numbers. "bi" operates all pixels,
"bE" is, Δx=bE*(1-X/1366), 0<X(integer)<1367.
"bN" is, Δy=bN*(1-Y/768), 0<Y(integer)<769.
X and Y are the number of pixels (natural number) from the left and top edges. Thus, we get a final brightness;
Y'(x,y)=Y(x,y)+Δx+Δy.
The Y'() is sames for RGB-components, and it can exceed the 8-bit range. In that case, following threshold is used.
IF(Y'()<0)Y'()=0, and IF(Y'()>255)Y'()=255.
Since Y'() is real number, finally we get,
Y"(x,y,R)=int{Y'(x,y,R)+0.5},
Y"(x,y,G)=int{Y'(x,y,G)+0.5}, ...
Those parameters are gathered, and it are written as "bi=bi,bE,bN".

5.5 Clouds

Since meteorological satellites observe clouds, the brightness of clouds is high. We exclude the bright clouds, when we want to get information on sea/ground surfaces than that of clouds. We use a threshold "C", and cut-off processing is done;
Y(x,y,average)={Y(x,y,R)+Y(x,y,G)+Y(x,y,B)}/3,
IF(Y(x,y,avarage)>C){Y(x,y,R)=0,Y(x,y,G)=...}.
At the same time, the "C" is defined a parameter, when "C>256" is inputted, non cut-off processing is executed.

The process of "Y ()=0" means that nothing is done at the pixel position (x, y).
When there are multiple images in time series {Y (..., t0), Y (..., t1), ..}, and the clouds move, the cutoff process may be able to detect patterns below the clouds.
For the possibility, a counter is attached to each pixel to record how many images are accumulated. After accumulating them, the pixel value is divided by the counter value, and we obtain the averaged brightness as one accumulated image. In this way, clouds can be erased to some extent.

The parameters in Sections 5.1-5.5 are related each other. Pay particular attention to 3 parameters of "bi=...". Please learn the feeling while actually operating them.

5.6 Moving objects

We need to Identify moving / non-moving patterns within a defined time interval. This is required to predict property of the detected pattern. We express 2 images as **Y**0 and **Y**1, which obtained at timing (t0, t1). Δt=t1-t0.
If the Δt is negligible, since the difference of brightness between the two images is less, "Δ**Y**=abs(**Y**0-**Y**1)" indicates moving patterns.
When the Δ**Y** image is calculated actually, it is Δ**Y** ~ **0** at Δt=10min. By using "amp=3,1,0, bi=110,0,0", the 0 value pixels are raised closer to the median value 127, and average brightness is amplified 3 times. We save the processed image in png-format. It is desirable to enhance the contrast of the png-image with a commercial available image editor. It is so pale images.
The images have edges of moving clouds. The edge-normal indicates the moving direction of clouds. Clouds do not have a clear outline in a storm. In that case, no edge lines are visible and the clouds become a dark, dispersed area image. Using character of this image, we can detect wind direction of typhoon paddlewheels and storms near the eyes. We call Δ**Y** "abs(sub)" image. The plain accumulation image is "P**Y**=(**Y**0+**Y**1)/2". "F**Y**=P**Y**-Δ**Y**" corresponds with non-moving patterns. We call F**Y** "alternative accumulation" image. Many kinds of phenomenon is understood by using FY and abs(sub) images.

6. Vortex

In our blog, many images of typhoons are published. At the junior/high school stage, descriptions of the typhoon represent a storm zone by a flat circle. In the circle, winds flow as a vortex; and there is a structure called the eye in the center. TV weather forecast reports that way.

Large-scale vortexes on Earth are counter clockwise in

the northern hemisphere and the reverse in the southern hemisphere. This is because of the Coriolis force works. Those descriptions are correct; we wish to get more advanced knowledgement about vortexes in the typhoon.

It is the best approach to understand the typhoon by using satellite images. Using the parameters described in Section 5, we make many kinds of typhoon images and track them, as for clouds formation sequence, flow, and changes of the central eyes. Then, you can see the individuality of typhoons. The individuality is (1) with or without eyes, (2) detailed cloud structure and temporal changes in the eyes, and (3) dust flow on the ground caused by winds around a typhoon.

Now let's consider the center of a vortex. The vortex transports surrounding matters to the center. So what happens to the transported ones? A 2-dimensional vortex would be a flow to another dimension (if it is exist). The typhoon is 3-dimensional. But, since it is phenomenon in the troposphere, the height is ~10 km, and even the medium size one has a diameter of 1000 km. Therefore, it is approximately a 2-dimensional vortex. Therefore, there is a vertical updraft flow at the center.

Is the updraft flow like a thin beam?

Satellite images of the typhoon show that the center is a circular ring having a diameter. It's size can be detected from a satellite, and it is stable during several days. Then, the updraft flow is not one beam. There is no singularity in the center. This cannot be understood with elementary knowledge of the vortex.

Only 2 types of stationary and axisymmetric vortexes in infinite space are possible: Burgers and Sullivan vortexes. The detail discussion was published in reference [12]. Since it is described by Japanese; we translate the important introduction part. Using the view point of following note, the typhoon is Sullivan vortex.

The Burgers and Sullivan vortexes spread over the entire 3D space, and their kinetic energies are both infinite. By redistributing that energy, it seems possible at any time to continuously change the flow from one to another. Intuitively, it seems that there is a path of continuous deformation from one to other, and that it is possible to satisfy the equation while changing the boundary conditions of the equation. Is it true that it cannot be done? If true, what's wrong with the intuition?

For details, please refer to the original note. From the original 3D streamline diagram, it can be seen that the central diameter of the typhoon may expand due to outward forces. The author wishes to consider the nebula vortex also.

Typhoons and swirling galaxies are both vortexes, but typhoon energy is much smaller than galaxies. In some galaxies, a small area in the center glows brightly. This unusually bright central object is called the active galactic nucleus (AGN). Its center is only 10^{-3} to 10^{-5} of diameter of the galaxy in size. The brightness is as bright as or more than entire galaxy [13].

Considering those knowledge, there is a small region in the center of spiral galaxies, which has a unique state. Then; is the spiral galaxy Burgers vortex? Spiral galaxies are 3D eddy, but they are near flat. In that case, there would be a material beam (in this case, a cluster of stars) in the center perpendicular to the galactic plane, but there are few such galaxies. Sometimes, there are galaxies with beams, but the beams are electromagnetic waves (light or X-ray), not material flows. Why is this?

We read ISAS's News [13], we find that there is a possibility of the black hole in the center of galaxies. If it exists, the material is sucked into the singularity and no beam is detected.

And, when absorbed by the singularity, the structural system of particles under normal gravity is destroyed, and beams of matter and energy (in this case, electromagnetic waves or neutrinos) blow out in the opposite direction of the flow of matter.

Let's terminate the deduction, because it's beyond the scope of environmental science. Please, understand that environmental science is an introduction to deeper, scientific knowledge.

After the typhoon has passed, vortexes of blue tide are often found on sea surface. It is prominent in oceans southeast and south of Australia. These vortexes have left/right directions, even though they are in the Southern Hemisphere. We wrote about those facts and the reason.

7. Yellow sand

Recently, the Mongolia region is going dryness (over grazing); therefore, the scale of yellow sand (Asian dust*) is increasing year by year. 2021, January 11th, the dust storm generated at 14:00 near the eastern end-western corridor of the Taklimakan desert and Jiuquan city. After 16:00, it expanded like an avalanche phenomenon, and at 17:00 it spread throughout Gansu province and inner Mongolia autonomous region. Dust storms can be confirmed by satellite images, that is, rather than being called yellow sand.

*) Asian dust looks yellow to brown. Even in Australia, the

dust phenomenon exists during typhoons. The dust looks red on Himawari-8. You can see the phenomenon that the red mist-like diffused image advances on sea surface.
The sandstorm passed through Shanxi to Shandong on the 12th, Shandong to the Liaodong peninsula on the 13th; and the mainstream dust front on the 14th passes Beijing. The tip has reached Seoul. On the 15th, it reached Hokkaido, Akita-Iwate, Miyagi-Fukushima prefectures in Japan. From the satellite image, it can be confirmed as a dark brown diffused fog.

However, the SPM and PM2.5 of the AEROS atmospheric measurement stations have hardly risen. The concentration is also low on the ground yellow sand map analyzed by JMA. It is probable that the yellow sand passed over the sky. A blue sea surface can be seen between the two streams on the south side. Even if SPM concentration on the ground is low, if they are much in upper sky; we believe there is "air pollution" in a global environment. SPM observation in the sky can be sampled by aircraft, but it is too costly. Currently it is the rider (ryder). If that is not possible, it is emission-less photoelectric observation. Generally available DB of SPM concentration in upper layers is unknown.

It is unusual for such a large-scale yellow sand phenomenon to occur in winter. Through image tracking of the yellow sand phenomenon, it can be confirmed that marine is polluted off the coast of Shanghai/ in the Bohai Bay and East China Sea have progressed since 2019. Global environmental destruction is underway on land and sea.

8. PM2.5

We consider the PM2.5 concentration, here. By a definition, it is the concentration of particles with a diameter size of 2.5 μm or less [μg/m^3].
It is an index related to yellow sand, but it does not correspond with 1: 1. The material of PM2.5 is not always silicate. PM2.5 increases as industrial activity flourishes. It costs to reduce the amount of dusts produced.

The particle size of yellow sand has a distribution. The median size flying to Japan is 4 μm. Elementary textbooks writes, "Solid particles in air fall off immediately." That is a true in case of stationary air. In nature, there are always up/down-drafts in the atmosphere. If the wind speed in upper layer is higher than that of ground, the field has an updraft. Particles of 8 μm or less don't fall unless they encounter a downward flow.

The PM2.5 concentration on the ground (altitude around 10m) has been measured and published as AEROS [10]. COVID-19 has affected industrial activity of each country. It is said that the amount of PM2.5 has decreased and the atmosphere has become cleaner. Is that true? We check with AEROS data.

Table 1 is PM2.5 concentrations at Beijing, Chengdu, Canton,
Shanghai, Shenyang, Seoul, Pusan, Jeju, and Tokyo in 2020.

Table 1. PM2.5 average concentration [μg/m^3] in 2020.

	data#	effective	defect	PM2.5
Beijing	8784	8445	339	39.3
Chengdu	8784	4537	4247	45.3
Canton	8784	8262	522	22.4
Shanghai	8784	8073	711	29.9
Shenyang	8784	8302	482	45.3
Seoul	8784	7542	1242	19.2
Pusan	8784	7526	1258	15.9
Jeju	8784	7424	1360	14.8
Tokyo	8556	8306	249	9.3

For comparison, the PM2.5 in 2018 and 2019 are shown in Tables 2 and 3.

Table 2. PM2.5 average concentration [μg/m^3] in 2019.

	data#	effective	defect	PM2.5
Beijing	8760	8620	140	43.0
Chengdu	8760	8403	357	49.0
Canton	8760	8316	444	29.5
Shanghai	8760	8302	458	37.8
Shenyang	8760	7406	1354	47.6
Seoul	8760	0	8760	?
Pusan	8760	0	8760	?
Jeju	8760	0	8760	?

Table 3. PM2.5 average concentration [μg/m^3] in 2018.

	data#	effective	defect	average
Beijing	8760	8468	292	50.2
Chengdu	8760	8408	352	51.6
Canton	8760	8511	249	32.3
Shanghai	8760	7714	1046	38.3
Shenyang	8760	8266	494	42.9
Seoul	8760	8469	291	23.0
Pusan	8760	8509	251	23.3
Jeju	8760	8421	339	19.1

The annual average is lower in 2020 than that of 2019 certainly.
But, the 2019 is even less than 2018. We believe that the decline is due to changes in industrial structures and technological innovations. The points to keep in mind when performing those calculations are as follows.
1) Outliers (values > 985) are considered "defect".

2) The defect is “no data”.

3) Measurement is every hour. If there are significant values before and after the no data, it is replaced by the average before and after.

4) The annual average is the sum of the significant divided by the number.

Next, we check a time series change of PM2.5. Setting unit time is important for detecting the effects of COVID-19. Human social activity is 1 week. The SARS-CoV-2 virus is said to take up to 2 weeks to develop. We adopt the 2-week unit, and the horizontal (x) axis is a reference time (Q-number) from Sunday to the 2nd Saturday. The correspondence table between Q-number and calendar is found in appendix. Thus; we get Figure 1.

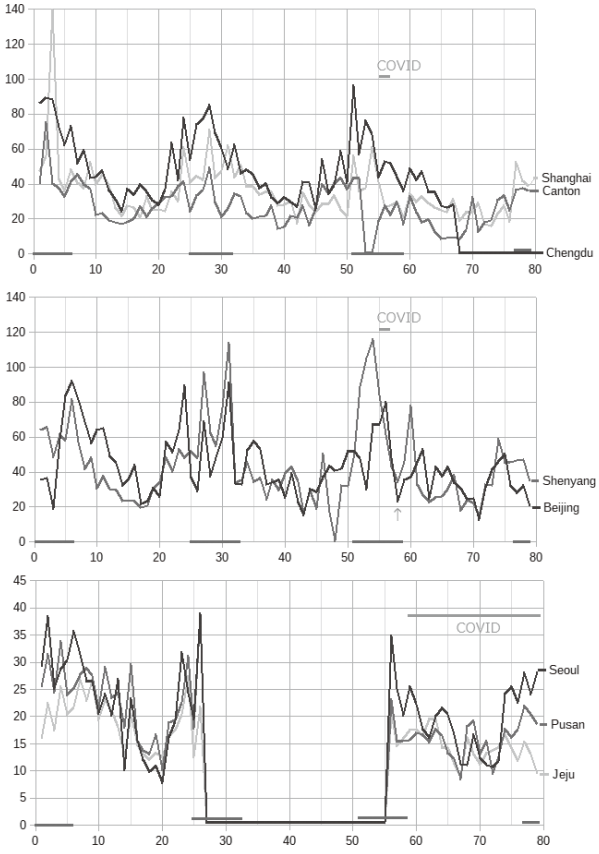

Figure 1. PM2.5 from 2018.1.1~2020.12.31, on China and south-Korea. Long-term missing data in south Korea is really erased from the DB.

Horizontal axis is the Q-number that is listed in Appendix 1. Vertical axis is PM2.5 concentration [μg/m^3].

Blue lines above horizontal axis is winter seasons** (12/1~3/15). Orange lines are the period when many* COVID patients are reported. *) 800 cases/d in China. **) the definition is in Appendix 1. In Figure 1, the effect of COVID is a sharp decrease in “Q=58” indicated by an orange arrows in Beijing and Shenyang. There is nothing else. So we extend the period to 1 season. The definition of seasons is in Appendix 1. Depending on the year, it is off by several days from the calendar. Since the period is about 3 months, the off-set of several days is ignored.

You must not calculate statistics by crossing the boundary of the days of a week. By the crossing, the effect of social activities varies from year to year.

The result is in Appendix 2. *Air purification due to reduced economic activity under COVID-19 could not be detected by using PM2.5 index*.

The section is described as an example to get into a quantitative discussion of environmental pollution from sky images.

9. Conclusion

Our blog is updated still now. Once you’ve visited and find images of interesting phenomenon, download the original and think about what and where the blog image is emphasized.

In the next step, you need to download the required measurements from DBs of quantitative measurements of the phenomenon, and process the data statistically; especially, calculate time series changes. Then, you should obtain physical and chemical knowledge that expresses phenomena from thesis and books. “Interest in images” is not education/research but an introduction. From those introductions, please be going to consider environmental phenomena.

References, Acknowledgements:

[1] About satellite image of **Himawari-8:**
Image courtesy: National Institute of Information and Communications Technology (NICT).
https://himawari8.nict.go.jp; https://himawari.asia/

[2] Meteorological data are in HP (https://www.jma.go.jp/jma/index.html) of Japan Meteorological Agency (**JMA**); They are free for academic and educational purpose. *Thank you very much for kindness of JMA.*
Yellow sand: http://www.data.jma.go.jp/gmd/env/kosa/fcst/fcst-s_as.html

[3] About satellite image of **SOHO**:
Solar and heliospheric observatory (SOHO); SOHO is a project of international cooperation between ESA and NASA.
SDO (Solar Dynamic Observatory), https://sdo.gsfc.nasa.gov/data/
SOHO Publications Acknowledgment writes that:
SOHO has an open data policy. When publishing a paper using SOHO data, please acknowledge SOHO as follows, (omit). We accept those.

[4] Image processing method: Academic repository "**Informatio** Vol.15-17" in University of Edogawa, Japan; https://edo.repo.nii.ac.jp/index.php

[5] **COVID** statistics:
https://www.worldometers.info/coronavirus/
Hannah Ritchie, "Coronavirus Source Data" in **Our World in Data** HP, https://ourworldindata.org/coronavirus-source-data; Thank you very much, Dr. Hannah Ritchie! Your data are *useful* very much for educational persons.

[6] Aerial photograph (1): Hydrographic and Oceanographic Department in Japan Coast Guard (**JCG**), https://www1.kaiho.mlit.go.jp/GIJUTSUKOKUSAI/kaiikiDB/kaiyo18-e1.htm

[7] Aerial photograph (2): **Geospatial Information Authority of Japan**, https://www.gsi.go.jp/
The Library: http://geolib.gsi.go.jp/map_search/results?lat=XXXX&lon=YYYY

[8] **Weather map**: //www.hbc.co.jp/weather/pro-weather.html

[9] 2nd source of Typhoon: Naval Oceanography Portal, **Joint Typhoon Warning Center**, https://www.metoc.navy.mil/jtwc/jtwc.html

[10] **SPM** concentration data: Ministry of the Environment, Japan, Atmospheric Environmental Regional Observation System (**AEROS**), http://soramame.taiki.go.jp/

[11] The blog is open to the public from 7/14, 2020. https://scienceimg140e.fc2.net/
Since it exists on a free server, it contains extra advertisements. Ignore it and ask for viewing, please.
There are many images in articles, but they are thumbnails in order to speed up brawzing. If you want to get more details, click them to enlarge please. Even if it is still insufficient, please download it.

[12] Koichi TAKAHASHI, "research note: About the Vortex Paradox", from Tohoku Gakuin University, Tenjinzawa, Izumi-ku, Sendai, Japan, 981-3193, https://www.tohoku-gakuin.ac.jp/research/journal/bk2015/pdf/no04_07.pdf.

[13] VLBI index, http://wwwj.vsop.isas.jaxa.jp/yougo/k01_agn.html.
Seiji KAMENO, "Active galactic nucleus 3C 84 jet and radio robe", ISAS (Institute of space and astronutical science) News, 1999.8, No.221. http://www.isas.ac.jp/docs/ISASnews/No.221/tokushuu-10.html

[14] We recommend machine translation services, http://translate.fuwhatsoft.com/

Appendix 1: Q-number and Calendar

Year	Date		Q#	season
2018	1/1	Mon	1	winter 2018
2018	1/14	Sun	2	winter 2018
2018	1/28	Sun	3	winter 2018
2018	2/11	Sun	4	winter 2018
2018	2/25	Sun	5	winter 2018
2018	3/11	Sun	6	winter 2018
2018	3/25	Sun	7	spring
2018	4/8	Sun	8	spring
2018	4/28	Sun	9	spring
2018	5/6	Sun	10	spring
2018	5/20	Sun	11	spring

2018	6/3	Sun	12	spring
2018	6/17	Sun	13	spring
2018	7/1	Sun	14	summer
2018	7/15	Sun	15	summer
2018	7/29	Sun	16	summer
2018	8/12	Sun	17	summer
2018	8/26	Sun	18	summer
2018	9/9	Sun	19	summer
2018	9/23	Sun	20	autumn
2018	10/7	Sun	21	autumn
2018	10/21	Sun	22	autumn
2018	11/4	Sun	23	autumn
2018	11/18	Sun	24	autumn
2018	12/2	Sun	25	winter 2019
2018	12/16	Sun	26	winter 2019
2018	12/30	Sun	27	winter 2019

Year	Date		Q#	
2019	1/13	Sun	28	winter 2019
2019	1/27	Sun	29	winter 2019
2019	2/10	Sun	30	winter 2019
2019	2/24	Sun	31	winter 2019
2019	3/10	Sun	32	winter 2019
2019	3/24	Sun	33	spring
2019	4/7	Sun	34	spring
2019	4/21	Sun	35	spring
2019	5/5	Sun	36	spring
2019	5/19	Sun	37	spring
2019	6/2	Sun	38	spring
2019	6/16	Sun	39	spring
2019	6/30	Sun	40	summer
2019	7/14	Sun	41	summer
2019	7/28	Sun	42	summer
2019	8/11	Sun	43	summer
2019	8/25	Sun	44	summer
2019	9/8	Sun	45	summer
2019	9/22	Sun	46	autumn
2019	10/6	Sun	47	autumn
2019	10/20	Sun	48	autumn
2019	11/3	Sun	49	autumn
2019	11/17	Sun	50	autumn
2019	12/1	Sun	51	winter 2020
2019	12/15	Sun	52	winter 2020
2019	12/29	Sun	53	winter 2020

Year	Date		Q#	
2020	1/12	Sun	54	winter 2020
2020	1/26	Sun	55	**COVID**
2020	2/9	Sun	56	**COVID**
2020	2/23	Sun	57	winter 2020
2020	3/8	Sun	58	winter 2020
2020	3/22	Sun	59	spring
2020	4/5	Sun	60	spring
2020	4/19	Sun	61	spring
2020	5/3	Sun	62	spring
2020	5/17	Sun	63	spring
2020	5/31	Sun	64	spring
2020	6/14	Sun	65	spring
2020	6/28	Sun	66	summer
2020	7/12	Sun	67	summer
2020	7/26	Sun	68	summer
2020	8/9	Sun	69	summer
2020	8/23	Sun	70	summer
2020	9/6	Sun	71	summer
2020	9/20	Sun	72	autumn
2020	10/4	Sun	73	autumn
2020	10/18	Sun	74	autumn
2020	11/1	Sun	75	autumn
2020	11/15	Sun	76	autumn
2020	11/29	Sun	77	winter 2021
2020	12/13	Sun	78	winter 2021
2020	12/27	Sun	79	winter 2021

Appendix 2: Changes of PM2.5 per the season

Winter				
position	Year	PM2.5	#	ratio
Beijing	2018	54.3	6	
Beijing	2019	50.6	8	0.93
Beijing	2020	52	8	**1.03**
Chengdu	2018	78.7	6	
Chengdu	2019	66.4	8	0.84
Chengdu	2020	61.4	8	0.92
Canton	2018	44.6	6	
Canton	2019	31.9	8	0.72
Canton	2020	30.9	6	0.97
Shanghai	2018	61.7	6	
Shanghai	2019	49.5	8	0.80
Shanghai	2020	39.5	8	0.80
Shenyang	2018	63.3	6	
Shenyang	2019	67.5	8	1.07
Shenyang	2020	73.1	8	**1.08**
Seoul	2018	31.3	6	
Seoul	2019	29.3	2	0.94
Seoul	2020	26.8	3	0.91
Pusan	2018	27.4	2	
Pusan	2019	28.4	3	1.04
Pusan	2020	18	3	0.63
Jeju	2018	20.6	2	
Jeju	2019	17.2	3	0.83
Jeju	2020	17	3	0.99

Spring				
Beijing	2018	61.4	7	
Beijing	2019	42.7	7	0.70
Beijing	2020	39.6	7	0.93
Chengdu	2018	44.8	7	
Chengdu	2019	39.9	7	0.89
Chengdu	2020	39	7	0.98
Canton	2018	29.3	7	
Canton	2019	23.1	7	0.79
Canton	2020	19	7	0.82
Shanghai	2018	40.3	7	
Shanghai	2019	37.3	7	0.93
Shanghai	2020	28.3	7	0.76
Shenyang	2018	39.3	7	
Shenyang	2019	34.6	7	0.88
Shenyang	2020	36.9	7	**1.07**

Summer				
Beijing	2018	31.3	6	
Beijing	2019	27.1	6	0.87
Beijing	2020	28.2	6	1.04
Chengdu	2018	33.6	6	
Chengdu	2019	32.9	2	0.98
Chengdu	2020	27.3	6	0.83
Canton	2018	21.7	6	
Canton	2019	21.3	6	0.98
Canton	2020	14.5	6	0.68
Shanghai	2018	25.8	6	
Shanghai	2019	27.3	6	1.06
Shanghai	2020	25.3	6	0.93
Shenyang	2018	23.6	6	
Shenyang	2019	30.2	6	1.28
Shenyang	2020	24.7	6	0.82

Autumn				
Beijing	2018	57.6	5	
Beijing	2019	43.1	5	0.75
Beijing	2020	40.2	5	0.93
Chengdu	2018	49.8	5	
Chengdu	2019	45.4	0	0.91
Chengdu	2020	?	5	?
Canton	2018	34.9	5	
Canton	2019	39	5	1.12
Canton	2020	25.3	5	0.65
Shanghai	2018	35.3	5	
Shanghai	2019	27.6	5	0.78
Shanghai	2020	20.3	5	0.74
Shenyang	2018	44.8	4	
Shenyang	2019	32.9	5	0.73
Shenyang	2020	43.1	5	**1.31**